Title
Accurate determination of production data of the non-standard positron emitter 86Y via the 86Sr(p,n)-reaction

Journal
Radiochimica Acta, 108(9)

ISSN
0033-8230

Authors
Uddin, M Shuza
Scholten, Bernhard
Basunia, M Shamsuzzhoha
et al.

Publication Date
2020-09-01

DOI
10.1515/ract-2020-0021

Peer reviewed

Rapid communication

M. Shuza Uddin, Bernhard Scholten, M. Shamsuzzhoha Basunia, Sandor Sudár, Stefan Spellerberg, Andrew S. Voyles, Jonathan T. Morrell, Haleema Zaneb, Jesus A. Rios, Ingo Spahn, Lee A. Bernstein, Bernd Neumaier and Syed M. Qaim*

Accurate determination of production data of the non-standard positron emitter ^{86}Y via the ^{86}Sr(p,n)-reaction

https://doi.org/10.1515/ract-2020-0021
Received March 16, 2020; accepted May 3, 2020; published online July 13, 2020

Abstract: In view of several significant discrepancies in the excitation function of the ^{86}Sr(p,n)$^{86g+xm}$Y reaction which is the method of choice for the production of the non-standard positron emitter ^{86}Y for theranostic application, we carried out a careful measurement of the cross sections of this reaction from its threshold up to 16.2 MeV at Forschungszentrum Jülich (FZJ) and from 14.3 to 24.5 MeV at LBNL. Thin samples of 96.4% enriched $^{86}SrCO_3$ were prepared by sedimentation and, after irradiation with protons in a stacked-form, the induced radioactivity was measured by high-resolution γ-ray spectrometry. The projectile flux was determined by using the monitor reactions ^{nat}Cu(p,xn)^{62,63,65}Zn and ^{nat}Ti(p,x)^{48}V, and the calculated proton energy for each sample was verified by considering the ratios of two reaction products of different thresholds. The experimental cross section data obtained agreed well with the results of a nuclear model calculation based on the code TALYS. From the cross section data, the integral yield of ^{86}Y was calculated. Over the optimum production energy range $E_p = 14 \rightarrow 7$ MeV the yield of ^{86}Y amounts to 291 MBq/μA for 1 h irradiation time. This value is appreciably lower than the previous literature values calculated from measured and evaluated excitation functions. It is, however, more compatible with the experimental yields of ^{86}Y obtained in clinical scale production runs. The levels of the isotopic impurities ^{87m}Y, ^{87g}Y, and ^{88}Y were also estimated and found to be <2% in sum.

Keywords: cross section; excitation function; integral yield and isotopic purity of the product; nuclear model calculation; proton irradiation; $^{86}SrCO_3$ thin sample.

1 Introduction

The positron-emitting radionuclide ^{86}Y ($T_{1/2}$ = 14.7 h) has been gaining increasing importance due to its theranostic application, i.e., its diagnostic use prior to the medication with the β^--emitting therapeutic radionuclide ^{90}Y ($T_{1/2}$ = 2.7 d). This concept was first applied at the Forschungszentrum Jülich (FZJ), Germany, in the context of treatment of a patient with disseminated bone metastases by using the therapeutic radionuclide ^{90}Y. A positron emission tomographic (PET) measurement of the injected ^{86}Y-citrate prior to therapy gave the distribution of the radioactivity in various organs, wherefrom the radiation dose caused by the subsequently administered therapeutic-agent ^{90}Y-citrate was quantitatively calculated [1]. Thereafter, the biodistributions of ^{86}Y-citrate and ^{86}Y-EDTMP (ethylene diamine tetramethylene phosphonate) were compared in several patients with prostate cancer [2]. A real impetus came after [^{90}Y]-DOTA-DPhe^1-Tyr^3-octreotide was found as a promising therapeutic agent and its radiation dosimetry in baboons was established with the help of ^{86}Y-labeled analog [3]. The concept was developed further; the progress achieved

***Corresponding author: Syed M. Qaim**, Institut für Neurowissenschaften und Medizin, INM-5: Nuklearchemie, Forschungszentrum Jülich, 52425 Jülich, Germany, E-mail: s.m.qaim@fz-juelich.de
M. Shuza Uddin: Institut für Neurowissenschaften und Medizin, INM-5: Nuklearchemie, Forschungszentrum Jülich, 52425 Jülich, Germany; Nuclear Science Division, Lawrence Berkeley National Laboratory, Berkeley, CA, 94720, USA; Tandem Accelerator Facilities, INST, Atomic Energy Research Establishment, Savar, Dhaka, Bangladesh
Bernhard Scholten, Stefan Spellerberg, Ingo Spahn and Bernd Neumaier: Institut für Neurowissenschaften und Medizin, INM-5: Nuklearchemie, Forschungszentrum Jülich, 52425 Jülich, Germany
M. Shamsuzzhoha Basunia, Andrew S. Voyles, Jonathan T. Morrell, Haleema Zaneb, Jesus A. Rios and Lee A. Bernstein: Nuclear Science Division, Lawrence Berkeley National Laboratory, Berkeley, CA, 94720, USA
Sandor Sudár: Institute of Experimental Physics, Debrecen University, Debrecen, 4001, Hungary

since then has been recently summarized [4]. The two radionuclides involved are called a "matched pair". Today, several other "matched pairs" are also known [5, 6]. They find application in many theranostic investigations.

For production of ^{86}Y several nuclear reactions were investigated (for a review cf. [7]). A critical consideration of those processes, however, led to the conclusion that the ^{86}Sr(p,n)^{86}Y reaction on a highly enriched target over E_p = 14 → 7 MeV is the most suitable route for the production of high-purity ^{86}Y. This low-energy process, originally developed by Rösch et al. [8, 9], is now the method of choice for the clinical scale production of ^{86}Y. Several laboratories contributed to production and efficient separation of ^{86}Y from the irradiated target cf. [9–20], so that this radionuclide has now been developed up to commercial scale production.

Despite the great success regarding the use of the ^{86}Sr(p,n)-reaction for the production of ^{86}Y, the existing nuclear reaction database contains discrepant data cf. [7, 21, 22]. Two measurements have been reported on ^{nat}Sr as target material [23, 24] and three on enriched ^{86}Sr [8, 25, 26]. For high-purity production of ^{86}Y, the data on enriched ^{86}Sr are more relevant. Out of the three reported works, two [8, 26] describe extensive data up to the proton energy of 18 MeV. One of those data sets [26], however, contains no details and the other [8] shows scattered values. A critical analysis based also on nuclear model calculations using three codes, namely ALICE-IPPE, TALYS and EMPIRE, revealed large discrepancies in the experimental data [7] and a new measurement was recommended [27]. This experimental study was therefore undertaken to provide an accurate set of data for this key production reaction. Some other competing reactions induced by protons on ^{86}Sr, e. g., ^{86}Sr(p,2n)^{85m,g}Y, which have thresholds beyond the energy range for the production of ^{86}Y, were also investigated. Similarly cross sections for the ^{86}Sr(p,n)^{86m}Y reaction were also measured. They are much smaller than those for the formation of ^{86g}Y. However, since the results for ^{85m,g}Y and ^{86m}Y are more of theoretical interest rather than for practical application, they will be reported later separately.

With regard to the radionuclidic purity of ^{86}Y, the ^{86}Sr(p,n)^{86}Y reaction on a highly enriched ^{86}Sr target is ideally suited for its production. However, since ^{86}Sr of 100% isotopic enrichment is not available, the radioactive products formed through (p,n) reactions on low-content ^{87}Sr and ^{88}Sr isotopes, present in the enriched target, also need to be considered. We therefore performed some experimental and evaluation studies on those reactions of secondary importance as well, and the results are given in an Appendix. Those data should allow a calculation of radionuclidic impurities in ^{86}Y while using an enriched ^{86}Sr target of any isotopic composition.

2 Experimental

2.1 Sample preparation and irradiations

Cross sections of proton induced reactions on enriched ^{86}Sr were measured by the stacked-sample activation technique. The enriched ^{86}Sr material was provided as $^{86}SrCO_3$ powder (isotopic composition: 96.4% ^{86}Sr; 1.33% ^{87}Sr; 2.26% ^{88}Sr; supplied by Eurisotop, France). Thin strontium carbonate samples were prepared at FZJ by the sedimentation technique [8, 10]. An Al foil of 50 μm thickness and 13 mm diameter (supplied by Good Fellow; chemical purity: 99.0%) was used after weighing as the backing for sedimentation. About 80 mg of the $^{86}SrCO_3$ powder was added to 6 mL toluene containing levapren-450 (1 mg/mL) to prepare a suspension. The levapren-450 has excellent film forming and adhesive properties and thus makes the sediment more stable on the backing. A 0.75 mL portion of the suspension was transferred to a 10 mm diameter hole of a sedimentation cell and then the solvent toluene was allowed to evaporate at room temperature. Two days were required for complete drying of the sediment. Thereafter, the $^{86}SrCO_3$ sediment with Al-backing was carefully removed from the cell and examined under a microscope. Only the homogeneous and mechanically stable samples were selected for irradiation. A photograph of two typical samples is shown in Figure 1. The exact diameter of each deposit and the weight of each sample were determined. The netto weight of the sediments lay in the range of 5 to 7 mg. From that weight the weight of levapren (0.75 mg) was subtracted. Each chosen sedimented sample was then covered by a 10 μm thick Al foil of 16 mm diameter welted around the backing foil; thus each $^{86}SrCO_3$ sediment sample was sandwiched between two Al-foils of different thicknesses.

Thin foils of Cu and Ti of natural isotopic composition (supplied by Good Fellow; purity: Cu (99.9%); Ti (>99.6%), thickness of both Cu and Ti foils: 25 μm) were cut in circular discs with a diameter of 13 mm. These foils were used as beam monitors. Four stacks were prepared with $^{86}SrCO_3$ sediment samples together with Cu and Ti foils inserted into the stack to follow the beam parameters along the stack.

Four irradiations of ^{86}Sr-containing stacks were carried out with protons. One irradiation with 27.0 ± 0.3 MeV primary energy protons was carried out for 30 min at a beam current of 100 nA at the 88-inch cyclotron, Lawrence Berkeley National Laboratory (LBNL), USA. The other three stacks were irradiated with 16.7 ± 0.2 MeV primary energy protons at the BC1710 cyclotron at FZJ, Germany, each for 30 min, and the beam current was kept constant at about 200 nA.

Figure 1: Photograph of two typical thin $^{86}SrCO_3$-sedimented layers (white circle) on Al backing whose uncovered part is dark.

2.2 Beam characterization

The extracted beam at the 88-inch cyclotron at Lawrence Berkeley National Laboratory (LBNL) is well characterized. The irradiation beam available at the solid target used in cross section measurements at the BC1710 at FZJ has also been well characterized [28]. The irradiated Cu monitor foil (25 μm thick) mounted in front of the stack was counted to determine the decay rate ratios of ^{63}Zn/^{62}Zn, ^{63}Zn/^{65}Zn, and ^{62}Zn/^{65}Zn formed in the same monitor foil [29, 30]. For this purpose, the activities of the three products, viz. ^{63}Zn ($T_{½}$ = 38.47 min), ^{62}Zn ($T_{½}$ = 9.19 h) and ^{65}Zn ($T_{½}$ = 244.93 d), were determined nondestructively by γ-ray spectrometry, extrapolated to the end of bombardment (EOB) and corrected for various factors (see below) to obtain the decay rates. The decay rate ratios of the above pairs were also calculated theoretically from the IAEA recommended excitation functions of the reactions ^{nat}Cu(p,x)^{63}Zn, ^{nat}Cu(p,x)^{62}Zn, and ^{nat}Cu(p,x)^{65}Zn, respectively [31]. The mean energy of the proton beam effective in the front Cu foil was determined by comparing the experimentally obtained ratio with the theoretical one. More details of the method have been reported earlier [28, 30].

2.3 Beam flux monitoring

During each irradiation, the beam current was measured by charge integration. It gave only an approximate value. The proton flux effective in the samples was also determined by activation of Cu and Ti monitors placed in front of a stack, whereby the ^{nat}Cu(p,x)^{62,63,65}Zn, and ^{nat}Ti(p,x)^{48}V reactions served as monitors. From the measured decay rates of ^{62,63,65}Zn and ^{48}V at EOB and the reference cross section of the respective monitor reaction taken from the IAEA evaluated data file [31], the proton flux was determined. The individual flux values from the above monitors agreed with one another within 6%. An average of those values was used to determine the cross section of the investigated reaction. This flux value was considered to be more accurate than that via charge integration. Besides flux measurement, the excitation functions of the three copper monitor reactions were also determined to check the beam parameters in the stack. The measured excitation functions reproduced well the recommended curves given by the IAEA [31]. This added high confidence to the various techniques used in our measurements. The computer program, STACK, written at FZJ and based on the energy-range relation [32], was utilized to determine the beam energy degradation along the stack.

2.4 Measurement of radioactivity and analysis

The radioactivity of the investigated radionuclides formed in Sr-samples and monitor foils was measured non-destructively using several high-purity germanium (HPGe) gamma-ray detectors associated with the necessary electronics and Maestro data acquisition software. The energy resolutions (FWHM) at 1332.5 keV of ^{60}Co of the HPGe detectors used were 1.9 keV at FZJ and 2.5 keV at LBNL. For efficiency calibration of the detectors standard point sources were used: at LBNL ^{54}Mn,^{133}Ba, ^{137}Cs, and ^{152}Eu, supplied by Isotope Products Laboratories, and at FZJ ^{22}Na, ^{54}Mn, ^{57}Co, ^{60}Co, ^{88}Y, ^{137}Cs, ^{152}Eu, ^{226}Ra, and ^{241}Am, supplied by Eckert & Ziegler, Berlin. The uncertainty in the activity of each source was specified as 3%. The γ-ray spectra measured in this work were analyzed by both the GammaVision and FitzPeaks [33] software. The counting was done repeatedly in several time segments depending on the half-life of the radionuclide. The ^{86g}Y radioactivity was measured after the decay of ^{86m}Y ($T_{½}$ = 48 min) to ^{86g}Y. Several measurements were done at a distance of 10 cm or 20 cm from the surface of the detector and the full decay curve was analyzed. Despite the large distance the effect of true coincident gamma ray summing was not negligible for the analyzed gammas of ^{86}Y because it has a complicated level scheme with numerous coincident transitions. The corrections were calculated with the TrueCoinc program [34]. Similarly, the ^{87g}Y activity was measured after disappearance of the 380.8 keV peak emitted in the decay of the metastable state ^{87m}Y ($T_{½}$ = 13.4 h). Since the radionuclides ^{87}Y ($T_{½}$ = 79.8 h) and ^{88}Y ($T_{½}$ = 106.65 d) were produced with proton induced reactions on the isotopic impurities ^{87}Sr (1.33%) and ^{88}Sr (2.26%), their activities were generally low. The counting of each sample was done about a week after EOB at a distance of 5 cm for 16 h. This provided good statistics for the observed radionuclides. The decay data of the investigated radionuclides were taken from the Lund/LBNL Nuclear Database [35] and are collected in Table 1. The decay and production data of the monitor reaction products were taken from [31].

2.5 Reaction cross section and its uncertainty

The peak area (counts) under a characteristic γ-ray of a reaction product was converted to count rate and extrapolated to the end of bombardment (EOB). This count rate was then converted to the decay rate by applying corrections for γ-ray intensity, efficiency of the detector, absorption and coincidence losses (random and real), if any. From this decay rate and the measured beam intensity, the cross

Table 1: Decay data of the investigated radionuclides[a].

Radionuclide	Production reaction	*Q*-value (MeV)	Half-life	γ-ray energy (keV)	γ-ray intensity (%)	True coincidence loss (%)
^{86g}Y	^{86}Sr(p,n)	−6.02	14.74(2) h	443.2	16.9(5)	1.34–4.59
	^{87}Sr(p,2n)	−14.45		627.7	32.6(10)	1.26–4.33
				1153.0	30.5(9)	1.30–4.39
^{87m}Y	^{87}Sr(p,n)	−3.02	13.37(3) h	380.8	78.0(1)	0
	^{88}Sr(p,2n)	−14.14				
^{87}Y	^{87}Sr(p,n)	−2.64	79.8(3) h	484.8	89.7(3)	0
	^{88}Sr(p,2n)	−13.76				
^{88}Y	^{88}Sr(p,n)	−4.40	106.65(4) d	898.0	93.7(3)	2.5
				1836.0	99.2(3)	2.5

[a]Taken from Lund/LBNL Nuclear Data Service (Chu et al., 1999) [35]. The latest decay data in the ENSDF database were checked through NuDAT available at www.nndc.bnl.gov and there was no significant difference. In parentheses, uncertainty is listed for the least significant digit(s).

section for the formation of the radioactive product was calculated using the usual activation formula. For ^{86}Y, all the γ-rays were analyzed. The final cross section value, however, was obtained by taking an average of the values from the three γ-rays given in Table 1.

The combined uncertainty in the cross section was estimated by taking the square root of the individual uncertainties in: peak area (1–2%), efficiency of the detector (5%), true coincidence correction (<2%), decay data, especially γ-ray intensities (<3%), proton flux (6%) and sample homogeneity (up to 5%). The overall uncertainty for ^{86}Y cross sections amounted to about 10% (1σ). The uncertainty originating from the particle flux inferred from the reference values of the monitor reactions dominates the overall uncertainty. In the case of subsidiary reaction products, namely ^{88}Y, ^{87m}Y, and ^{85g}Y, an additional uncertainty of <10% due to the low abundance of the respective target isotope was adopted. The uncertainty in the decay data of those radionuclides is, however, smaller than that for ^{86}Y. The overall uncertainty in the cross sections of the three subsidiary reactions thus amounted to about 14% (1σ).

3 Nuclear model calculation

The reaction cross sections were calculated using the nuclear model code TALYS [36] version 1.4, to avoid the energy shift mentioned in ref [22]. TALYS incorporates several nuclear models to calculate all the significant nuclear reaction mechanisms over the energy range of 1 keV to 200 MeV. In the calculations, the particle transmission coefficients were generated via the spherical optical model using the ECIS-06 code [37] with global parameters: for neutrons and protons from Koning and Delaroche [38]; for the optical model parameters (OMP) of complex particles (d, t, α, ^{3}He) the code made use of a folding approach, building up the OMPs from the neutron and proton potential. The parameters of OM were modified for protons and neutrons to get the best description of the experimental data. The gamma-ray transmission coefficients were calculated through the energy-dependent gamma-ray strength function according to Kopecky and Uhl [39] for E1 radiation, and according to Brink [40] and Axel [41] for all the other transition types. For the pre-equilibrium reactions, a two-component exciton model of the TALYS code was used. The energies, spins, parities and branching ratios of the discrete levels were based on the RIPL-3 database [42]. In some cases, the energies, spins, parities and branching ratios of the discrete levels were modified based on the information in the literature [43]. In the continuum region, the level density was calculated by the back-shifted Fermi gas model [44] using its slightly modified version in TALYS [45]. For the ratio of the effective moment of inertia to the rigid body moment of inertia ($\Theta_{eff}/\Theta_{rig}$) parameter of the spin distribution of the level density, the systematics based on the evaluation by Sudár and Qaim [46] was used.

The fit of the nuclear reaction model calculation to the experimental data was checked by the reduced χ^2 analysis. With the appropriate parameters, a reduced χ^2 of 1.25 was achieved for the measured data of the ^{86}Sr(p,n)$^{86g+xm}$Y reaction reported in this work.

4 Results and discussion

4.1 Activation cross sections related to the production of ^{86}Y

The radionuclide ^{86}Y has two isomeric states; the short-lived metastable state ^{86m}Y ($T_{1/2}$ = 48 min) and the relatively longer lived ground state ^{86g}Y ($T_{1/2}$ = 14.74 h). The metastable state decays 99.31% by isomeric transition to the ground state and 0.69% by EC. The ^{86m}Y activity was measured immediately after the end of irradiation, and the ^{86g}Y activity after complete decay of ^{86m}Y. The measured cross section is a sum of the ^{86}Sr(p,n)$^{86m+g}$Y processes: $\sigma_{g+xm} = \left(\sigma_g + P_m \frac{\lambda_m}{\lambda_m - \lambda_g}\sigma_m\right)$ [47], where P_m is the probability of the isomeric transition to the ground state. The factor x is calculated as 1.055. The ^{86}Y was formed via two direct proton induced nuclear reactions, one on the enriched target ^{86}Sr and the other on the impurity ^{87}Sr. The contribution of the ^{87}Sr(p,2n)^{86}Y (E_{th} = 14.62 MeV) was corrected from the cross section ratios of σ(p,n)/(σ(p,n)+σ(p,2n)) obtained theoretically and by considering the abundance level of ^{87}Sr (1.33%) in the enriched ^{86}Sr target. In the energy range above 15 MeV, the contribution of the (p,2n) reaction was found to be between 2 and 10% of the measured values. An uncertainty of about 10% in that correction was included in the reported cross section.

The cross sections measured in this work are given in Table 2 and are also shown as a function of proton energy in Figure 2; the results obtained at LBNL are denoted by solid black circles and those at FZJ by solid red circles. The data measured in the two laboratories agree well in the overlapping energy region. This demonstrates the reliability of various techniques used in the determination of the experimental data in the two laboratories.

The literature data for this reaction, based on measurements on the enriched ^{86}Sr targets, are also shown in Figure 2. Rösch et al. [8] reported values which are about 1.5–2 times higher than the present measurements. A large uncertainty is associated with those measured values. In particular, about 10% uncertainty each was involved in the target thickness and beam intensity determination. The statistical uncertainty was between 10 and 20%. On the other hand, the systematically higher values indicate a missing common parameter of cross section determination. Presumably the efficiency of the detector or the proton flux was

Table 2: Measured cross sections for the production of ^{86}Y via the ^{86}Sr(p,n)-process.

Proton energy (MeV)	Cyclotron	Measured cross section (mb)
24.5 ± 0.4	88-inch	53 ± 5[a]
22.5 ± 0.4		60 ± 6[a]
20.5 ± 0.4		147 ± 15[a]
18.4 ± 0.5		288 ± 29[a]
17.0 ± 0.5		440 ± 44[a]
15.7 ± 0.5		556 ± 56[a]
14.3 ± 0.5		604 ± 51
16.2 ± 0.2	BC1710	544 ± 54[a]
16.0 ± 0.2		506 ± 51[a]
14.7 ± 0.2		594 ± 51
14.3 ± 0.2		574 ± 48
13.4 ± 0.3		571 ± 49
13.0 ± 0.3		601 ± 50
12.0 ± 0.3		570 ± 48
11.0 ± 0.3		527 ± 44
10.5 ± 0.3		472 ± 40
9.6 ± 0.4		415 ± 35
8.8 ± 0.4		362 ± 30
8.3 ± 0.4		323 ± 27
7.9 ± 0.4		290 ± 24
6.9 ± 0.4		143 ± 12
6.5 ± 0.4		100 ± 9

[a]A small contribution (<10%) of the ^{87}Sr(p,2n)$^{86m+g}$Y reaction on the 1.33% ^{87}Sr present in the enriched ^{86}Sr target was corrected (see text). The extra uncertainty due to this correction is included in the total uncertainty of the reported cross section value.

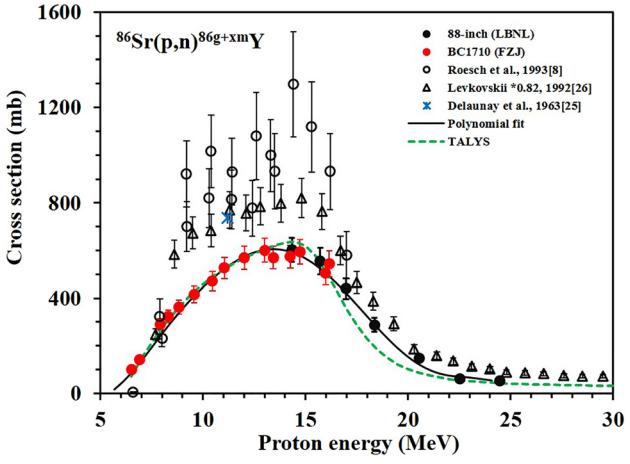

Figure 2: Excitation function for the formation of the radionuclide ^{86}Y in proton irradiation of an enriched ^{86}Sr target.

not properly determined. A normalization of those data is therefore not possible. The data reported by Levkovskii [26] are also too high. However, they could be scaled down by 18% due to correction for the monitor reaction cross section [47]. The reduced data are also shown in Figure 2. Those values are still much larger than the present measurements. The estimated uncertainty in those values amounts to 12%.

In Figure 2 we give also the results of the nuclear model calculation described above. The present experimental data are reproduced very well by the model calculation; this adds confidence to our new measurements. The TALYS can thus describe correctly the measured data with appropriate model parameters.

4.2 Integral yield of ^{86}Y

We fitted the new experimental data with a polynomial function of the fifth order. The fitted curve is almost exactly the same as the results of the model calculation. The fitted curve (see Figure 2) was then used to calculate the integral yield of ^{86}Y, assuming 100% enrichment of the target nuclide ^{86}Sr and an irradiation time of 1 h at a proton beam current of 1 μA cf. [48]. The results are shown in Figure 3 as a function of the incident proton energy and, because of their practical importance, they are also given in a tabular form (Table 3). A comparison of the integral yield of ^{86}Y calculated from the present cross section data over $E_p = 14 \rightarrow 7$ MeV with the values available in the literature [7, 8, 21, 22] is given in Table 4. Similar to this work, Rösch et al. [8] had calculated the yield from their experimental data. The other three values, however, have been derived from the evaluated curves. Qaim et al. [21] and Zaneb et al. [7] considered all data points, the latter presenting a very critical and detailed evaluation of all available data in the literature. The third evaluation recently reported by Tárkányi et al. [22] is very empirical. Our calculated yield values are considerably lower than the previously reported values.

Zaneb et al. [7] also performed a critical comparison of the experimental integral yields of ^{86}Y obtained by several authors [10, 12, 14, 15, 18] with the reported calculated yields [7, 8, 21, 22]. They found that the experimental yields ranged between 43 and 88% of the theoretical values. With the new accurate measurement of the excitation function in this work, and therefrom the calculated integral yield of ^{86}Y, the gap between the experimental and calculated values has considerably decreased. For example, in the detailed production experiment by Kettern et al. [10], involving a 4 h irradiation at a proton current of 5 μA, the reported experimental yield of ^{86}Y after chemical separation now amounts to about 87% of the yield calculated from the present excitation function, which is very satisfactory.

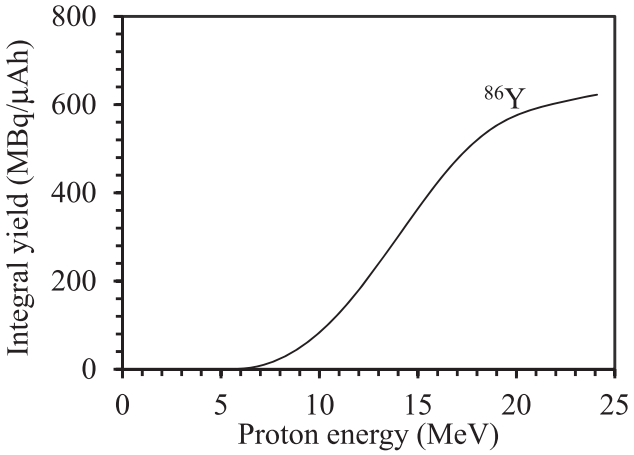

Figure 3: Integral yield of the radionuclide ^{86}Y calculated from the measured excitation function of the ^{86}Sr(p,n)-process, assuming an irradiation time of 1 h at a proton beam current of 1 μA. The data are shown as a function of the proton energy.

Table 3: Calculated integral yield of ^{86}Y formed via the ^{86}Sr(p,n)-process.

Proton energy (MeV)	Integral yield of ^{86}Y (MBq/μAh)[a]	Proton energy (MeV)	Integral yield of ^{86}Y (MBq/μAh)[a]
6.0	1.5	16.0	430
7.0	9.0	17.0	480
8.0	24	18.0	520
9.0	47	19.0	552
10.0	89	20.0	575
11.0	132	21.0	592
12.0	183	22.0	601
13.0	241	23.0	613
14.0	300	24.0	622
15.0	375		

[a]Calculated assuming an irradiation time of 1 h at a proton beam current of 1 μA.

4.3 Isotopic impurities in ^{86}Y

In the production of ^{86}Y, the non-isotopic impurities, i. e., the radionuclides of Sr and Rb formed, are easily removed by a chemical separation, and the formation of the isotopic impurities ^{85m}Y and ^{85g}Y via the ^{86}Sr(p,2n)-reaction is avoided by keeping the incident proton energy below 14 MeV. Due to its short half-life the level of ^{86m}Y activity is high but most of it decays to ^{86g}Y by the time the separated product comes to medical application. On the other hand, due to the lack of availability of a 100% enriched ^{86}Sr target, proton induced reactions on Sr-isotopes of masses other than 86, present in low abundances in the enriched ^{86}Sr target, lead to the radioactive impurities ^{87m}Y, ^{87g}Y, and ^{88}Y via the ^{87}Sr(p,n)^{87m}Y, ^{87}Sr(p,n)^{87g}Y, and ^{88}Sr(p,n)^{88}Y reactions, respectively. In the Appendix we give the calculated integral yields of those reaction products as a function of proton energy. From those curves the levels of the three radioactive impurities expected in the ^{86g}Y produced were calculated, taking into account the abundances of ^{87}Sr (1.33%) and ^{88}Sr (2.26%) present in the enriched ^{86}Sr target and assuming an irradiation time of 1 h. The results are given in Table 4. They are comparable with the experimental values reported by Rösch et al. [9] and recently by Aluicio-Sarduy et al. [20], as well as with the calculated values from the evaluated curves by Zaneb et al. [7]. This shows that although the cross section data reported by Rösch et al. [8] were high, their activity ratio measurements [9] were correct, which are independent of absolute values of detector efficiency and particle flux. In the production of ^{86}Y, the major impurity appears to be ^{87m,g}Y at a level of < 2%. This has been experimentally confirmed by a few other groups as well. It is also pointed out that the level of ^{87m}Y impurity in ^{86g}Y will remain more or less constant due to their similar half-lives. The levels of ^{87g}Y and ^{88}Y impurities in ^{86g}Y will, however, increase with decay time due to their longer half-lives. Presumably, the levels of the three

Table 4: Calculated integral yields of ^{86}Y and the associated isotopic radionuclidic impurities.

	Energy range (MeV)	^{86}Y yield (MBq/μAh)[a]	Impurity (%)				
			^{85m}Y	^{85g}Y	^{87m}Y	^{87g}Y	^{88}Y
This work	14 → 7	291	ND	ND	1.25	0.09	0.02
Rösch et al. [8]	14 → 7	475	<0.001[c]	<0.001[c]	1.4[c]	0.2[c]	0.06[c]
Aluicio-Sarduy et al. [20]	14 → 7				1.62[d]	0.27[d]	0.12[d]
Qaim et al. evaluation [21][b]	14 → 7	433					
Tárkányi et al. evaluation [22][b]	14 → 7	374					
Zaneb et al.evaluation [7][b]	14 → 7	371			1.5–3.0	0.4–0.5	

[a]Yield calculated from the assuming an irradiation time of 1 h at a proton beam current of 1 μA.
[b]Evaluated data based on older measurements.
[c]Impurities determined experimentally [9].
[d]Impurities determined experimentally [20].

isotopic impurities would be considerably reduced if ^{86}Sr of ~99% enrichment could be used as target material.

5 Conclusion

Through an accurate measurement of the excitation function of the ^{86}Sr(p,n)$^{86m+g}$Y reaction, the discrepancies in the existing data up to 17 MeV have been removed and the database has been strengthened up to 24 MeV. The integral yield of ^{86}Y over $E_p = 14 \rightarrow 7$ MeV, calculated from the present excitation function, amounts to 291 MBq/μA for 1 h irradiation time. It is much lower than the previously reported values, calculated from the other experimental or evaluated excitation functions. The present value is, however, closer to the experimentally determined production yields of ^{86}Y as well as to its integral yield calculated from the TALYS curve reported in this work. An accurate estimation of the isotopic impurities ^{87m,g}Y and ^{88}Y showed that >98% pure ^{86}Y is produced using the 96.4% enriched ^{86}Sr target. The level of the impurity would be considerably reduced if ~99% enriched target could be made available.

Acknowledgments: M. S. Uddin thanks the Alexander von Humboldt (AvH) Foundation in Germany and Lawrence Berkeley National Laboratory, USA, for financial support. He would also like to acknowledge the authorities of Bangladesh Atomic Energy Commission and Ministry of Science and Technology, Dhaka, Bangladesh, for granting leave of absence to conduct these experiments abroad. H. Zaneb thanks the LBNL and the Higher Education Commission (HEC) of Pakistan for the opportunity and support to conduct a piece of research abroad while doing her Ph.D. work at the Physics Department of Government College University Lahore, Pakistan. We all thank the operation crews of the cyclotron BC1710 at FZJ and 88-inch cyclotron at LBNL for their help in irradiation of samples. The work at LBNL was performed under the auspices of the U.S. Department of Energy under contract No. DE-AC02-05CH11231. This research is supported by the U.S. Department of Energy Isotope Program, managed by the Office of Science for Nuclear Physics.
Author contribution: All the authors have accepted responsibility for the entire content of this submitted manuscript and approved submission.
Research funding: M. S. Uddin thanks the Alexander von Humboldt (AvH) Foundation in Germany and Lawrence Berkeley National Laboratory, USA, for financial support.
Conflict of interest statement: The authors declare no conflicts of interest regarding this article.

Appendix

Formation cross sections and integral yields of the isotopic impurities ^{87m}Y, ^{87g}Y and ^{88}Y

During the measurements on the ^{86}Sr(p,n)$^{86g+xm}$Y reaction described above, cross sections of three subsidiary reactions, namely ^{87}Sr(p,n)^{87m}Y, ^{87}Sr(p,n)^{87g}Y and ^{88}Sr(p,n)^{88}Y, leading to the isotopic impurities ^{87m}Y, ^{87g}Y and ^{88}Y, respectively, were also measured. The data obtained for only 1.33% abundant ^{87}Sr and 2.26% abundant ^{88}Sr in the enriched ^{86}Sr were extrapolated to 100% abundance each, and the results are given in Appendix Table 1. The extrapolation of results for the ^{88}Sr(p,n)^{88}Y reaction was straightforward because no other reaction contributes to the formation of ^{88}Y. In the case of the ^{87}Sr(p,n)^{87m}Y and ^{87}Sr(p,n)^{87g}Y reactions, however, extrapolation was appropriate only up to 14 MeV. Beyond that energy range, corrections for the contributions of the ^{88}Sr(p,2n)^{87m,g}Y processes were necessary. We applied those corrections by using the evaluated data reported by Zaneb et al. [7]. The extrapolated data for ^{88}Y agreed with the results of two previous careful measurements [10, 24] in which $^{nat}SrCO_3$ samples (with ^{88}Sr abundance of 82.58%) were used as targets. This added confidence to our present measurement.

For constructing the excitation function of the ^{88}Sr(p,n)^{88}Y reaction, we adopted the basic diagram by Zaneb et al. [7] and added the new data [24 and this work] to it. A polynomial function was then fitted to all the concordant points and the curve thus obtained was used for the yield calculation. For the ^{87}Sr(p,n)^{87m}Y reaction, three sets of data exist in the literature [10, 24, 26]. Our data agree

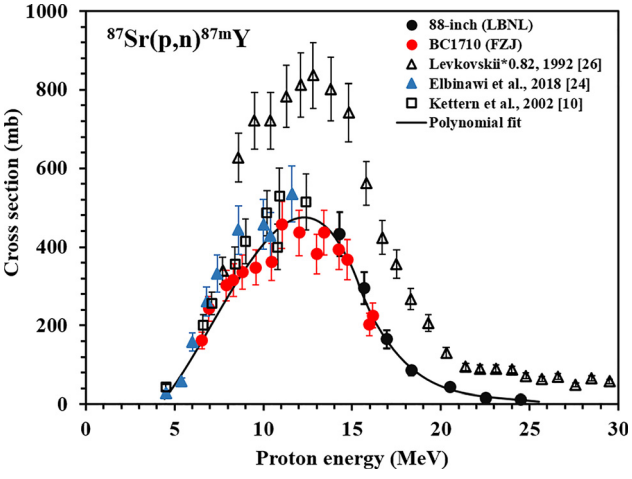

Appendix Figure 1: Excitation function of the ^{87}Sr(p,n)^{87m}Y reaction.

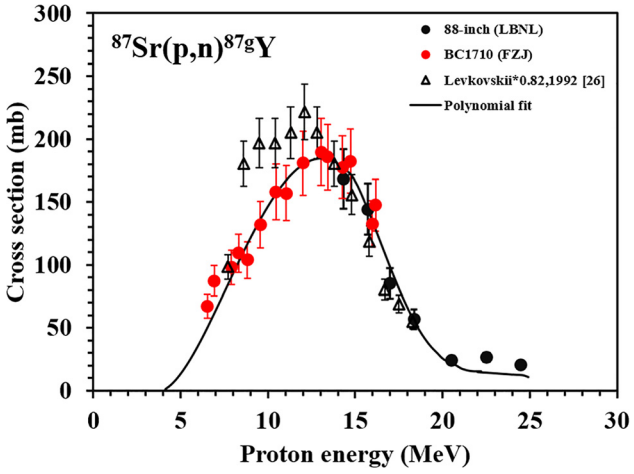

Appendix Figure 2: Excitation function of the ^{87}Sr(p,n)^{87g}Y reaction. The data describe the independent formation cross sections of ^{87g}Y.

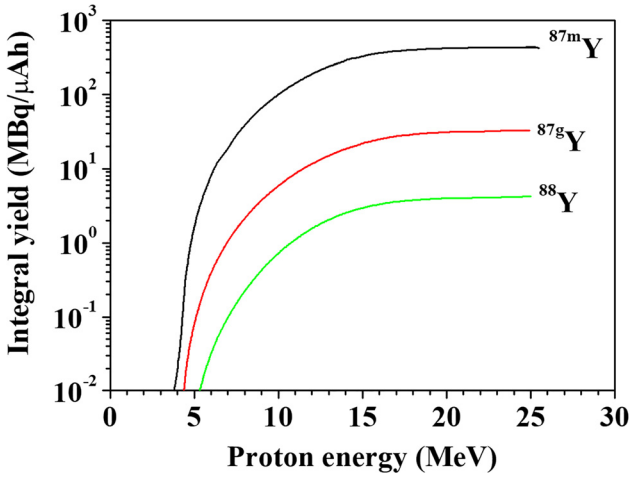

Appendix Figure 3: Integral yields of the radionuclides ^{87m}Y, ^{87g}Y and ^{88}Y, calculated from the measured excitation functions of the ^{87}Sr(p,n)^{87m}Y, ^{87}Sr(p,n)^{87g}Y and ^{88}Sr(p,n)^{88}Y processes, assuming 100% abundance of the target isotope and an irradiation time of 1 h. The curves are shown as a function of the proton energy.

very well with the values by Kettern et al. [10] and Elbinawi et al. [24] but not with Levkovskii [26] (cf. Appendix Figure 1). A polynomial fit through the three concordant datasets [10, 24], and [this work] gave the required curve for the yield calculation. The data for the ^{87}Sr(p,n)^{87g}Y reaction are shown in Appendix Figure 2. They describe the independent formation of ^{87g}Y, i. e., without any contribution from the decay of ^{87m}Y. In this case a polynomial fit through own data points was carried out.

From the fitted excitation functions of the above mentioned three reactions, the integral yields of ^{87m}Y, ^{87g}Y and ^{88}Y were calculated for 100% abundance of the target isotope, assuming a 1 h irradiation with a proton beam current of 1 μA. The result is given in Appendix Figure 3.

Appendix Table 1: Cross sections for the formation of isotopic impurities ^{87m}Y, ^{87g}Y and ^{88}Y.

Proton energy (MeV)	Cyclotron	Measured cross sections (mb)		
		^{87}Sr(p,n)^{87m}Y	^{87}Sr(p,n)^{87g}Y[a]	^{88}Sr(p,n)^{88}Y
24.5 ± 0.4	88-inch	12 ± 1.6	20 ± 3	47 ± 7
22.5 ± 0.4		15 ± 2	26 ± 4	51 ± 7
20.5 ± 0.4		44 ± 6	24 ± 3	96 ± 14
18.4 ± 0.5		85 ± 12	57 ± 8	221 ± 31
17.0 ± 0.5		165 ± 23	85 ± 12	376 ± 53
15.7 ± 0.5		296 ± 41	144 ± 20	606 ± 86
14.3 ± 0.5		433 ± 56	168 ± 24	656 ± 86
16.2 ± 0.2	BC1710	225 ± 32	147 ± 21	472 ± 62
16.0 ± 0.2		203 ± 28	133 ± 19	456 ± 60
14.7 ± 0.2		368 ± 52	182 ± 26	716 ± 94
14.3 ± 0.2		394 ± 51	178 ± 25	720 ± 94
13.4 ± 0.3		436 ± 57	186 ± 26	859 ± 113
13.0 ± 0.3		382 ± 50	190 ± 27	884 ± 116
12.0 ± 0.3		435 ± 57	181 ± 25	835 ± 110
11.0 ± 0.3		457 ± 59	157 ± 22	753 ± 99
10.5 ± 0.3		362 ± 47	158 ± 22	657 ± 86
9.6 ± 0.4		348 ± 45	132 ± 18	605 ± 79
8.8 ± 0.4		336 ± 44	104 ± 15	505 ± 66
8.3 ± 0.4		316 ± 41	109 ± 15	456 ± 60
7.9 ± 0.4		302 ± 39	98 ± 14	404 ± 53
6.9 ± 0.4		243 ± 32	87 ± 12	249 ± 33
6.5 ± 0.4		162 ± 21	67 ± 9	169 ± 22

[a]These cross sections are for independent formation of ^{87g}Y, i. e., without the contribution via the decay of ^{87m}Y.

Those data should allow calculation of the three radionuclidic impurities under consideration while using an enriched ^{86}Sr target of any isotopic composition.

References

1. Herzog H., Rösch F., Stöcklin G., Lueders C., Qaim S. M., Feinendegen L. E. Measurement of pharmacokinetics of ^{86}Y radiopharmaceuticals with PET and radiation dose calculation of analogous ^{90}Y radiotherapeutics. *J. Nucl. Med.* 1993, *34*, 2222–2226.
2. Rösch F., Herzog H., Plag C., Neumaier B., Braun U., Müller-Gärtner H. W., Stöcklin G. Radiation doses of yttrium-90 citrate and yttrium-90 EDTMP as determined via analogous yttrium-86 complexes and positron emission tomography. *Eur. J. Nucl. Med.* 1996, *23*, 958–966.
3. Rösch F., Herzog H., Stolz B., Brockmann J., Köhle M., Mühlensiepen H., Marbach P., Müller-Gärtner H. W. Uptake kinetics of the somatostatin receptor ligand [^{86}Y]DOTA-DPhe^{1}-Tyr^{3}-octreotide ([^{86}Y]SMT487) using positron emission tomography in non-human primates and calculation of radiation doses of the ^{90}Y-labelled analogue. *Eur. J. Nucl. Med.* 1999, *26*, 358–366.
4. Rösch F., Herzog H., Qaim S. M. The beginning and development of the theranostic approach in nuclear medicine, as exemplified by the radionuclide pair ^{86}Y and ^{90}Y. *Pharmaceuticals* 2017, *10*, 1–28.

5. Qaim S. M., Scholten B., Neumaier B. New developments in the production of theranostic pairs of radionuclides. *J. Radioanal. Nucl. Chem.* 2018, *318*, 1493–1509.
6. Qaim S. M. Theranostic radionuclides; recent advances in production methodologies. *J. Radioanal. Nucl. Chem.* 2019, *322*, 1257–1266.
7. Zaneb H., Hussain M., Amjed N., Qaim S. M. Nuclear model analysis of excitation functions of proton induced reactions on 86Sr, 88Sr and natZr: Evaluation of production routes of 86Y. *Appl. Radiat. Isot.* 2015, *104*, 232–241.
8. Rösch F., Qaim S. M., Stöcklin G. Nuclear data relevant to the production of the positron emitting radioisotope 86Y via the 86Sr(p,n)- and natRb(3He,xn)-processes. *Radiochim. Acta* 1993, *61*, 1–8.
9. Rösch F., Qaim S. M., Stöcklin G. Production of the positron emitting radioisotope ^{86}Y for nuclear medical application. *Appl. Radiat. Isot.* 1993, *44*, 677–681.
10. Kettern K., Linse K. H., Spellerberg S., Coenen H. H., Qaim S. M. Radiochemical studies relevant to the production of ^{86}Y and ^{88}Y at a small-sized cyclotron. *Radiochim. Acta* 2002, *90*, 845–849.
11. Reischl G., Rösch F., Machulla H. J. Electrochemical separation and purification of yttrium-86. *Radiochim. Acta* 2002, *90*, 225–228.
12. Garmestani K., Milenic D. E., Plascjak P. S., Brechbiel W. W. A new and convenient method for purification of ^{86}Y using a Sr(II) selective resin and comparison of biodistribution of ^{86}Y and ^{111}In labelled Herceptin™. *Nucl. Med. Biol.* 2002, *29*, 599–606.
13. Park L. S., Szajek L. P., Wong K. J., Plascjak P. S., Garmestani K., Googins S., Eckelman W. C., Carrasquillo J. A., Paik C. H. Semi-automated ^{86}Y purification using a three column system. *Nucl. Med. Biol.* 2004, *31*, 297–301.
14. Yoo J., Tang L., Perkins T. A., Rowland D. J., Laforest R., Lewis J. S., Welch M. J. Preparation of high specific activity ^{86}Y using a small biomedical cyclotron. *Nucl. Med. Biol.* 2005, *32*, 891–897.
15. Avila-Rodriguez M. A., Nye J. A., Nickles R. J. Production and separation of non-carrier-added ^{86}Y from enriched ^{86}Sr targets. *Appl. Radiat. Isot.* 2008, *66*, 9–13.
16. Lukic D., Tamburella C., Buchegger F., Beyer G. J., Comor J. J., Seimbille Y. High efficient production and purification of ^{86}Y based on electrochemical separation. *Appl. Radiat. Isot.* 2009, *67*, 523–529.
17. Kandil S. A., Scholten B., Hassan K. F., Hanafi H. A., Qaim S. M. A comparative study on the separation of radioyttrium from Sr- and Rb-targets via ion-exchange and solvent extraction techniques, with special reference to the production of no-carrier-added ^{86}Y, ^{87}Y and ^{88}Y using a cyclotron. *J. Radioanal. Nucl. Chem.* 2009, *279*, 823–832.
18. Sadeghi M., Aboudzadeh M., Zali A., Boulourinovin F. Radiochemical studies relevant to ^{86}Y production via ^{86}Sr(p,n)^{86}Y for PET imaging. *Appl. Radiat. Isot.* 2009, *67*, 7–10.
19. Oehlke E., Hoehr C., Hou X. C., Hanemaayer V., Zeisler S., Adam M. J., Ruth T. J., Celler A., Buckley K., Benard F., et al. Production of ^{86}Y and other radiometals for research purposes using a solution target system. *Nucl. Med. Biol.* 2015, *42*, 842–849.
20. Aluicio-Sarduy E., Hernandez R., Valdovinos H. F., Kutyreff C. J., Ellison P. A., Barnhart T. D., Nickles R. J., Engle J. W. Simplified and automatable radiochemical separation strategy for the production of radiopharmaceutical quality ^{86}Y using single column extraction chromatography. *Appl. Radiat. Isot.* 2018, *142*, 28–31.
21. Qaim S. M., Tárkányi F., Capote R., Eds. *Nuclear Data for the Production of the Therapeutic Radionuclides*. Technical Reports Series No. 473; International Atomic Energy Agency: Vienna, 2011; pp. 1–377.
22. Tárkányi F., Ignatyuk A. V., Hermanne A., Capote R., Carlson B. V., Engle J.W., Kellett M. A., Kibédi T., Kim G. N., Kondev F. G., et al. Recommended nuclear data for medical radioisotope production: diagnostic positron emitters. *J. Radioanal. Nucl. Chem.* 2019, *319*, 533–666.
23. Michel R., Bodemann R., Busemann H., Daunke R., Gloris M., Lange H. J., Klug B., Krins A., Leya,I., Luepke M., et al. Cross sections for the production of residual nuclides by low and medium energy protons from the target elements C, N, O, Mg, Al, Si, Ca, Ti, V, Mn, Fe, Co, Ni, Cu, Sr, Y, Zr, Nb, Ba and Au. *Nucl. Instr. Methods B* 1997, *129*, 153–193.
24. Elbinawi A., Al-Abyad M., Bashter I., Seddik U., Ditroi F. Excitation function of proton induced nuclear reaction on strontium: Special relevance to the production of ^{88}Y. *Appl. Radiat. Isot.* 2018, *140*, 272–277.
25. Delaunay-Olkowsky J., Strohal P., Cindro N. Total reaction cross section of proton induced reactions. *Nucl. Phys.* 1963, *47*, 266–272.
26. Levkovskii V. N. *Activation Cross Sections for Nuclides of Average Masses (A=40–100) by Protons and Alpha-particles with Average Energies (E=10–50 MeV). Experiment and Systematics*; Inter-Vesy: Moscow, 1992, ISBN, 5-265-02732-7.
27. Qaim S. M. Nuclear data for production and medical application of radionuclides: present status and future needs. *Nucl. Med. Biol.* 2017, *44*, 31–49.
28. Spellerberg S., Scholten B., Spahn I., Bolten W., Holzgreve M., Coenen H. H., Qaim S. M. Target development for diversified irradiations at a medical cyclotron. *Appl. Radiat. Isot.* 2015, *104*, 106–112.
29. Piel H., Qaim S. M., Stöcklin G. Excitation functions of (p,xn)-reactions on ^{nat}Ni and highly enriched ^{62}Ni: Possibility of production of medically important radioisotope ^{62}Cu at a small cyclotron. *Radiochim. Acta* 1992, *57*, 1–5.
30. Uddin M. S., Chakraborty A. K., Spellerberg S., Shariff M. A., Das S., Rashid M. A., Spahn I., Qaim S. M. Experimental determination of proton induced reaction cross sections on ^{nat}Ni near threshold energy. *Radiochim. Acta.* 2016, *104*, 305–314.
31. Hermanne A., Ignatyuk A. V., Capote R., Carlson B. V., Engle J. W., Kellett M. A., Kibédi T., Kim G., Kondev F. G., Hussain M., et al. Reference cross sections for charged-particle monitor reactions. *Nucl. Data Sheets* 2018, *148*, 338–382.
32. Williamson C. F., Boujot J. P., Picard J. *Tables of Range and Stopping Power of Chemical Elements for Charged Particles of Energies from 0.5 to 500 MeV*. Report CEA-R 3042, 1966.
33. Fitzgerald J. JF Computing Services, 17 Chapel Road, Stanford in the Vale, Oxfordshire, SN7 8LE. Copyright © Jim Fitzgerald 1991-2016, Last updated 8th October 2016; https://jimfitz.co.uk.
34. Sudár S. *"TrueCoinc", a Software Utility for Calculation of the True Coincidence Correction. "Specialized Software Utilities for Gamma Ray Spectrometry"*, 1996–2000. IAEA-TECDOC-1275; p. 37.
35. Chu S. Y. F., Ekström L.P., Firestone R.B. *The Lund/LBNL Nuclear Data Search, Version 2.0*, February, 1999. https://nucleardata.nuclear.lu.se/toi/.

36. Koning A. J., Hilaire S., Duijvestijn, M. C. *Proceedings of the International Conference on Nuclear Data for Science and Technology*, April 22–27, 2007: Nice, France, 2007; pp. 211–214.
37. Raynal J. *Notes on ECIS94, CEA Saclay Reports*, vol. No. *CEA-N-2772*, 1994.
38. Koning A. J., Delaroche I. P. Local and global nucleon optical models from 1 keV to 200 MeV. *Nucl. Phys. A* 2003, *713*, 231–310.
39. Kopecky J., Uhl M. Test of gamma-ray strength functions in nuclear reaction model calculations. *Phys. Rev. C* 1990, *41*, 1941–1955.
40. Brink D. M. Individual particle and collective aspects of the nuclear photoeffect. *Nucl. Phys.* 1957, *4*, 215–220.
41. Axel P. Electric dipole ground-state transition width strength function and 7-MeV photon interactions. *Phys. Rev.* 1962, *126*, 671–683.
42. Capote R., Herman M. , Oblozinsky P., Young P., Goriely S., Belgya T., Ignatyuk A., Koning A. J., Hilaire S., Plujko V., et al. RIPL 3 reference input parameter library for calculation of nuclear reactions and nuclear data evaluations. *Nucl. Data Sheets* 2009, *110*, 3107.
43. Negret A., Singh B. Nuclear Data Sheets for A = 86. Nuclear Data Sheets 2015, 124-156, From ENSDF database as of 10 27, 2019. The version available at https://www.nndc.bnl.gov/ensarchivals/.
44. Dilg W., Schantl W., Vonach H., Uhl M. Level density parameters for the back-shifted Fermi gas model in the mass range 40 < A < 250. *Nucl. Phys. A* 1973, *217*, 269–298.
45. Koning A. J., Hilarie S., Goriely S. Global and local level density models. *Nucl. Phys. A* 2008, *810*, 13–76.
46. Sudár S., Qaim S. M. Mass number and excitation energy dependence of the $\Theta_{eff}/\Theta_{rig}$ parameter of the spin cut-off factor in the formation of an isomeric pair. *Nucl. Phys. A* 2018, *979*, 113–142.
47. Qaim S. M., Sudár S., Scholten B., Koning A. J., Coenen H. H. Evaluation of excitation functions of 100Mo(p,d+pn) 99Mo and 100Mo (p,2n)99mTc reactions: Estimation of long-lived Tc-impurity and its implication on the specific activity of cyclotron-produced 99mTc. *Appl. Radiat. Isot.* 2014, *85*, 101–113.
48. Otuka N., Takács S. Definitions of radioisotope thick target yields. *Radiochim. Acta* 2015, *103*, 1–6.